ARTICLE NO. 78-1082R

Aerodynamic Effects Induced by a Vectored High Aspect Ratio Nonaxisymmetric Exhaust Nozzle

Douglas L. Bowers*
Air Force Flight Dynamics Laboratory, Wright-Patterson Air Force Base, Ohio

Nonaxisymmetric exhaust nozzles exiting at or near the trailing edge of a lifting surface offer advanced aircraft configurations improved performance because of induced aerodynamic effects. An experimental investigation of these induced effects was conducted at Mach numbers from 0.3 to 0.9 on a half-span wing body configuration with a high aspect ratio vectoring (0, 15, 30 deg) nonaxisymmetric exhaust nozzle incorporated into the wing trailing edge. Results indicate that, at all Mach numbers, the thrust-removed lift, drag, and pitching moment coefficients for the wing body increased with increasing nozzle vectoring. Using the trimmed data, an optimum drag polar can be formed which uses all three vector angles. As the nozzle pressure ratio increases, the induced effects on the wing aerodynamics tend to increase proportionally.

Nomenclature

AR = model wing aspect ratio
AR_c = model canard aspect ratio
$b/2$ = model wing half span, in.
C_D = drag coefficient, D/qs
C_L = lift coefficient, L/qS
C_M = pitching moment coefficient at quarter chord, moment/$qS\bar{c}$
C_p = pressure coefficient, $(P-P_\infty)/q$
C_T = gross thrust coefficient, thrust, lb/qs
c_r = root chord, in.
c_t = tip chord, in.
$\bar{c}$ = mean aerodynamic chord
D = drag, lb
L = lift, lb
M = Mach number
NPR = nozzle pressure ratio, P_T/P_∞
P = local static pressure, psi
P_T = total pressure at nozzle throat, psi
P_∞ = freestream static pressure
S = model wing area, in.^{2}
S_c = model canard area, in.^{2}
q = dynamic pressure, psi
X/c = distance from wing leading edge in percent chord
$2Y/b$ = distance from wing root in percent span
α = angle of attack, deg
Λ_{LE} = leading edge wing sweep angle, deg
Λ_{TE} = trailing edge wing sweep angle, deg

Introduction

ANALYSIS of aircraft wing aerodynamics and aircraft propulsion system performance have for most aircraft systems been conducted as separate aspects of total aircraft performance. Exceptions to this trend include jet flap technology, laminar flow control research, and vertical/short takeoff configurations, where the propulsion system must be included as an integral part of aircraft aerodynamics. Although the technology developed in these exceptions has not been utilized in more than a few prototype aircraft systems, a new aerodynamics/propulsion related technology, the nonaxisymmetric exhaust nozzle, offers improved aircraft system performance which may have impact on advanced aircraft design for many years. Some of the benefits identified for nonaxisymmetric exhaust nozzles include 1) increased lift, attributed to induced aerodynamics created by the nozzle exhaust flow near the wing trailing edge; 2) increased instantaneous maneuver with a vectoring exhaust jet; 3) improved cruise performance due to reduced aftbody installation drag; 4) improved deceleration characteristics in-flight and on landing when utilizing a thrust reverser; and 5) reduced observables, i.e., radar cross-section and infrared signature.

While the last three benefits are related to nozzle/aftbody geometry and mechanical design, the first two benefits are directly related to a combination of wing aerodynamics and the exhaust nozzle jet. To realize these benefits, the exhaust nozzle exit should be at or near the wing trailing edge. The aircraft wing aerodynamics and the propulsion system performance, in this case, are not easily separated because the propulsion-induced effects on the aircraft lift, drag, and pitching moment coefficients can be significant. As shown in Fig. 1, the contribution of propulsion-induced lift can be as great as the jet thrust component in the lift direction. Figure 2 presents an example of an advanced aircraft configuration which utilizes propulsion-induced aerodynamics. Examples of previous research in this area have emphasized jet flaps,[2] over-the-wing blowing,[3,4] and integrated wing/exhaust nozzle configurations.[5,6]

The purpose of this investigation was to explore the induced and total performance aerodynamic coefficients (lift, drag, and pitching moment) for a wing/body configuration with a vectoring high aspect ratio nonaxisymmetric exhaust nozzle at the wing trailing edge. This paper describes the experimental investigation which utilized a half-span wind tunnel model which was fully metric and incorporated 0, 15, and 30 deg high aspect ratio vectoring exhaust nozzles.

Description of Aeropropulsion Model

The wind tunnel model utilized in this effort was available equipment at the Air Force Flight Dynamics Laboratory (AFFDL) Trisonic Gasdynamics Facility (TGF). The half-span model shown in Fig. 3, was a wing/body/canard configuration with interchangeable exhaust nozzles incorporated at the wing trailing edge near the wing root. The primary instrumentation was a five-component force balance which

Presented as Paper 78-1082 at the AIAA/SAE 14th Joint Propulsion Conference, Las Vegas, Nev., July 25-27, 1978; submitted Sept. 1, 1978; revision received Dec. 18, 1978. Copyright © American Institute of Aeronautics and Astronautics, Inc., 1978. All rights reserved. Reprints of this article may be ordered from AIAA Special Publications, 1290 Avenue of the Americas, New York, N.Y. 10019. Order by Article No. at top of page. Member price $2.00 each, nonmember $3.00 each. **Remittance must accompany order.**

Index categories: Airbreathing Propulsion; Aerodynamics; Performance.

*Aerospace Engineer. Member AIAA.

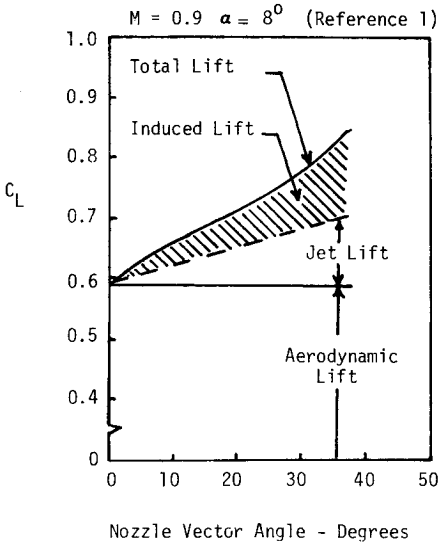

Fig. 1 Induced lift due to thrust vectoring.

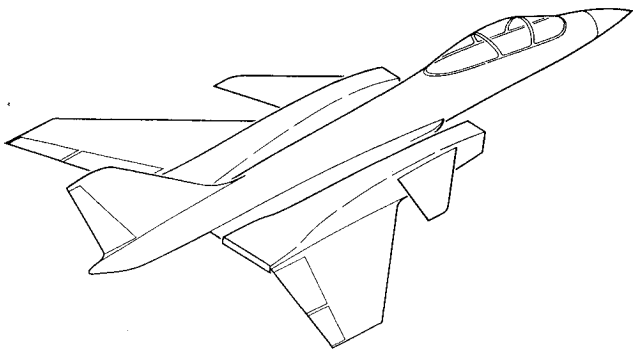

Fig. 2 Advanced aeropropulsion aircraft configuration.

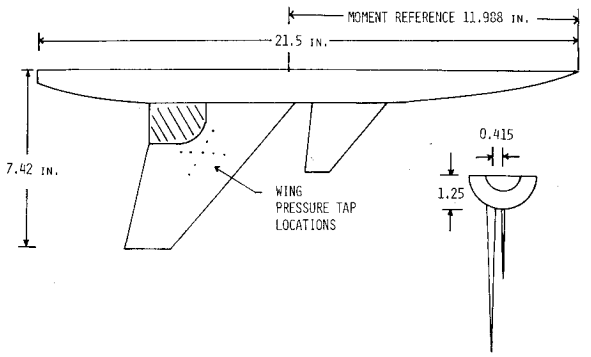

Fig. 3 Half-span test model (Ref. 7).

measured the forces on the entire model, primarily lift, drag, and pitching moment. The moment center for this model was at the quarter chord of the trapezoidal wing planform.

The wing planform had a leading edge sweep of 40 deg and a trailing edge sweep of 12.62 deg. The wing airfoil varied from a NACA 63A206 at the wing root to a NACA 65A204 at the wing tip. All wing parameters are based on the trapezoidal planform. The wing was instrumented with limited upper surface static pressure orifices near the area of influence for the exhaust nozzle flow.

A canard located on the fuselage forward and above the wing was also tested. The canard planform was approximately 39% of the wing surface area. Table 1 describes additional wing and canard planform parameters.

The nonaxisymmetric exhaust nozzles were convergent-type with a span that was approximately 29% of the wing span (from the wing-body junction). Cold high pressure air was

Table 1 Wing and canard planform characteristics[a]

	Wing	Canard
$b/2$	7.42 in.	2.867 in.
S	31.46 in.^{2}	12.18 in.^{2}
AR	3.5	2.765
$\bar{c}$	4.65 in.	2.254 in.
c_r	6.5237 in.	3.131 in.
c_t	1.9571 in.	1.017 in.
Λ_{LE}	40 deg	40 deg
Λ_{TE}	12.62 deg	5.37 deg
Airfoils		
Root	NACA 63A206	NACA 64A204
Tip	NACA 65A204	

[a] Data from Ref. 7.

used as a jet efflux. Vectoring of the convergent exhaust nozzles to the 15 and 30 deg positions was accomplished by turning the last 5% of the integrated nozzle. The effect of the nozzle surface being turned into the freestream flow, while not unlike some proposed advanced nonaxisymmetric exhaust nozzle vectoring schemes, is different from the vectoring mechanism used in Ref. 5. The aerodynamic effects of thrust vectoring in this test were not only due to induced effects but also due to the "flap" effect of the turned down nozzle. The vectored nozzle data in Ref. 5 was produced by turning vanes in the exhaust flow which produce larger lift increments with drag increments relatively smaller than those produced by other vectoring schemes. The "flap" effect in vectored exhaust nozzle performance will be discussed in another section. The aspect ratio of these nonaxisymmetric exhaust nozzles (defined as the ratio of the exhaust nozzle width to height at the nozzle throat) was approximately 11.0.

To separate the exhaust nozzle thrust from the total configuration forces, the exhaust nozzle, the body, and a small portion of the wing surface forward of the nozzle (shown cross-hatched in Fig. 3) were tested at static conditions at the scheduled nozzle pressure ratios with the wind tunnel pumped down to static pressures corresponding to the wind-on test Mach number conditions. The force balance measured the components of lift, drag, and pitching moment due to the thrust over an angle-of-attack range for the 0, 15, and 30 deg vectored nozzles. The static thrust force components were then subtracted from the wind-on full wing/body configuration data to obtain the thrust removed aerodynamic components.

Facility Description and Test Parameters

The Trisonic Gasdynamics Facility, located at Wright-Patterson Air Force Base, is a closed-circuit variable-density continuous-flow wind tunnel with an operating Mach number range of 0.23 to 3.00. Two test sections were utilized for this effort. For the subsonic Mach numbers from 0.3 to 0.7, the solid wall 2 by 2 ft test section was used with the half-span model mounted directly to a wall plate. A transonic test section, 15 by 15 in. square with slotted sidewalls top and bottom, was utilized for a portion of the 0.7 and all of the 0.8 and 0.9 Mach number data.

Nominal test parameters were 0.3 to 0.9 Mach numbers, nozzle pressure ratios from jet-off to maximum (determined by model stress limits), angles of attack from −4 deg to 15 deg, and a unit Reynolds number of 2.0×10^6/ft.

Aerodynamic Changes Due to Thrust Vectoring

The combined aerodynamic and propulsion forces for an aircraft constitute the total performance capability of that system. To realize the nonaxisymmetric exhaust nozzle benefit, the aircraft drag polars (total lift coefficient vs total drag coefficient) should indicate improvements while vectoring the thrust. Figures 4, 5, and 6 present powered polars for representative subsonic Mach numbers. All of the

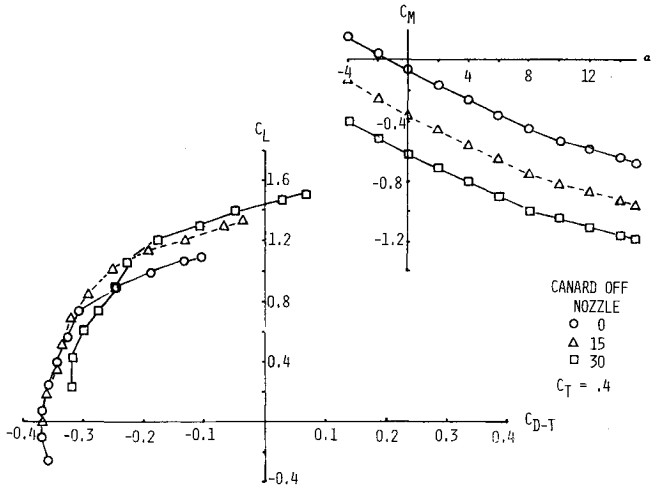

Fig. 4 Powered polar, $M=0.3$, $NPR=3$.

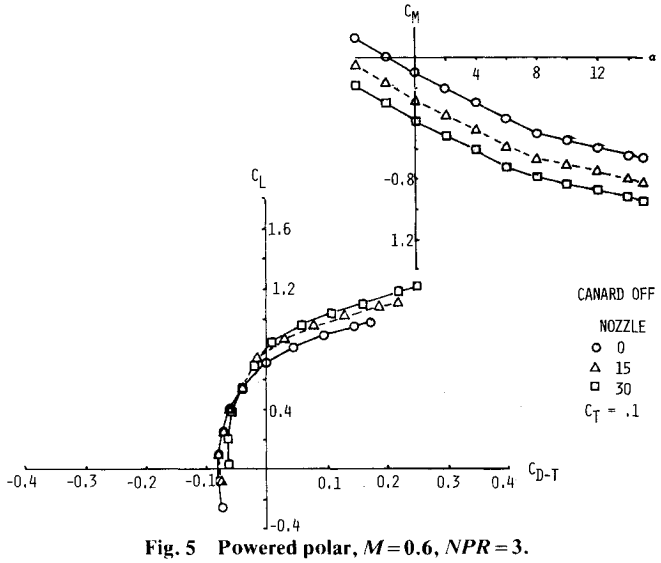

Fig. 5 Powered polar, $M=0.6$, $NPR=3$.

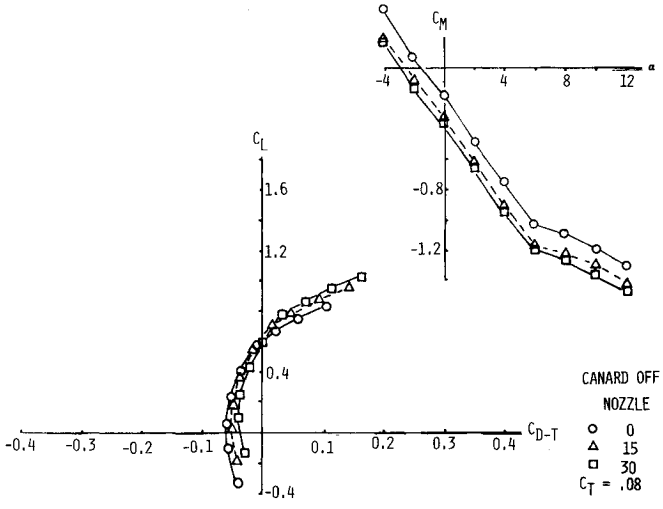

Fig. 6 Powered polar, $M=0.9$, $NPR=5$.

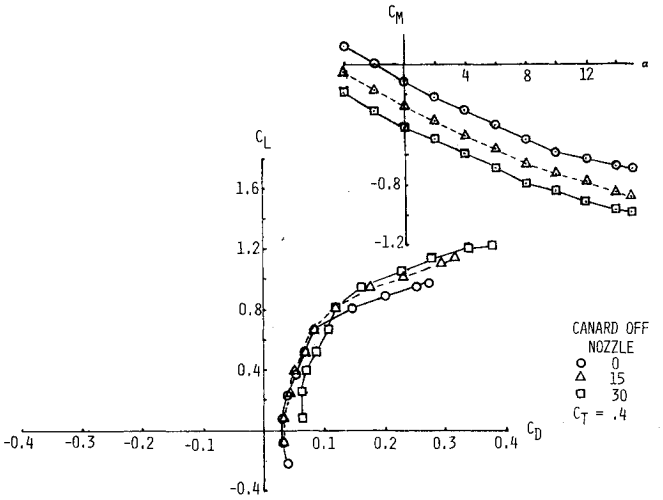

Fig. 7 Thrust-removed drag polar, $M=0.3$, $NPR=3$.

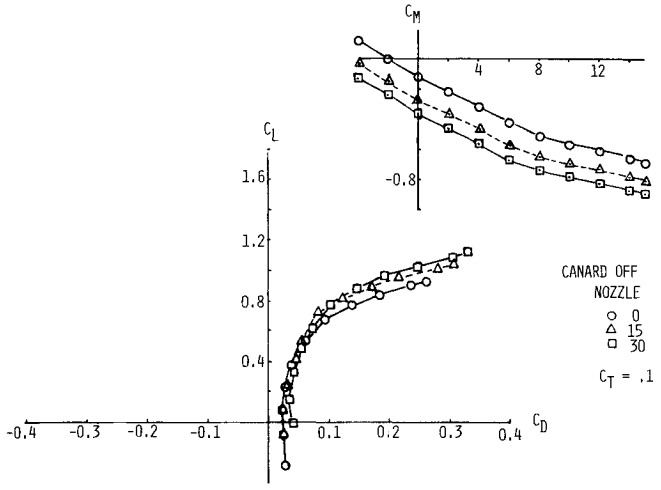

Fig. 8 Thrust-removed drag polar, $M=0.6$, $NPR=3$.

powered polars show the vectored exhaust nozzle polars crossing over the nonvectored exhaust nozzle polar. An optimum powered polar can be constructed, therefore, which takes advantage of all vector angles. As lift coefficient is increased, increasing the nozzle vector angle improves the polar. These changes in the polars with vectoring can be attributed to jet induced aerodynamic effects, a "flap" effect with the turned down nozzle surface, and a direct jet lift effect. This section will discuss these components as well as the effects of forward fuselage mounted canard and nozzle pressure ratio effects. The data presented for these nominal Mach numbers are representative of data taken in the tests at other Mach numbers.

The powered polars in these figures indicate benefits for thrust vectoring, especially at high angles of attack or high lift coefficients and at the lower Mach numbers 0.3 and 0.6. While this data is untrimmed, the change in the drag polar is not expected to negate the entire improvement. If the static jet lift (i.e., the component of lift due to the vectored exhaust flow) is removed, the induced aerodynamic effects and the "flap" effect remain. Thrust-removed drag polars for 0.3, 0.6 and 0.9 Mach numbers are shown in Fig. 7, 8 and 9. For the $M_\infty=0.3$ and 0.6 thrust-removed drag polars, a benefit is still evident for thrust vectoring up to 30 deg. Both vectored nozzle drag polars cross over the unvectored polar, and the 30 deg polar crosses the 15 deg polar. For the $M_\infty=0.9$ thrust-removed drag polar, however, the changes with vectored nozzles are very small, though the 15 and 30 deg vectored nozzle data does cross over the unvectored polar at high lift coefficient. The negligible change in the drag polar indicates small changes in the induced lift, drag, and pitching moment coefficients.

The benefits shown for thrust vectoring in Figures 7 and 8 for 0.3 and 0.6 Mach number are made up of induced aerodynamic effects and the nozzle surface "flap" effect. The

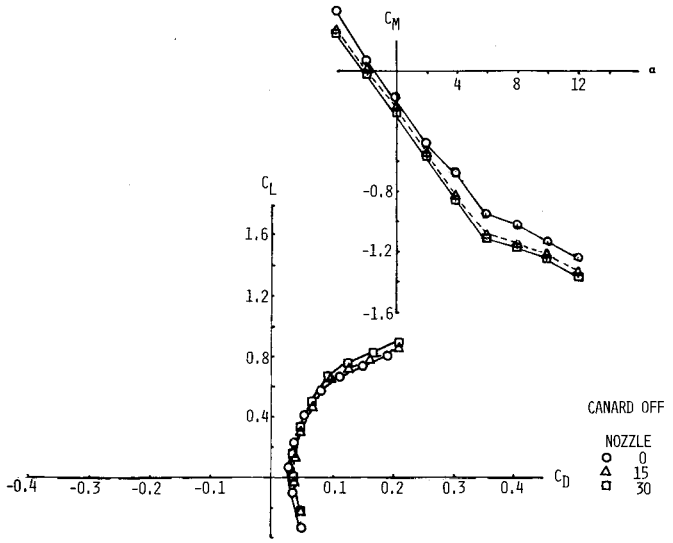

Fig. 9 Thrust-removed drag polar, $M=0.9$, $NPR=5$.

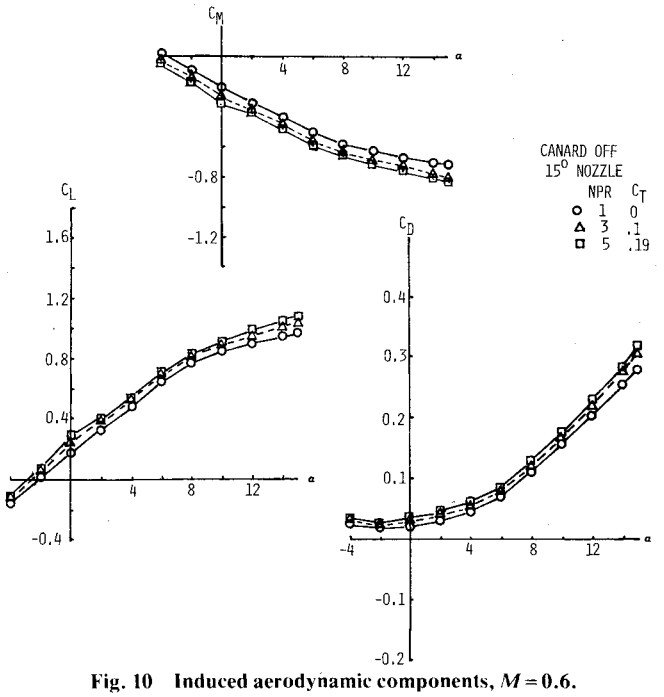

Fig. 10 Induced aerodynamic components, $M=0.6$.

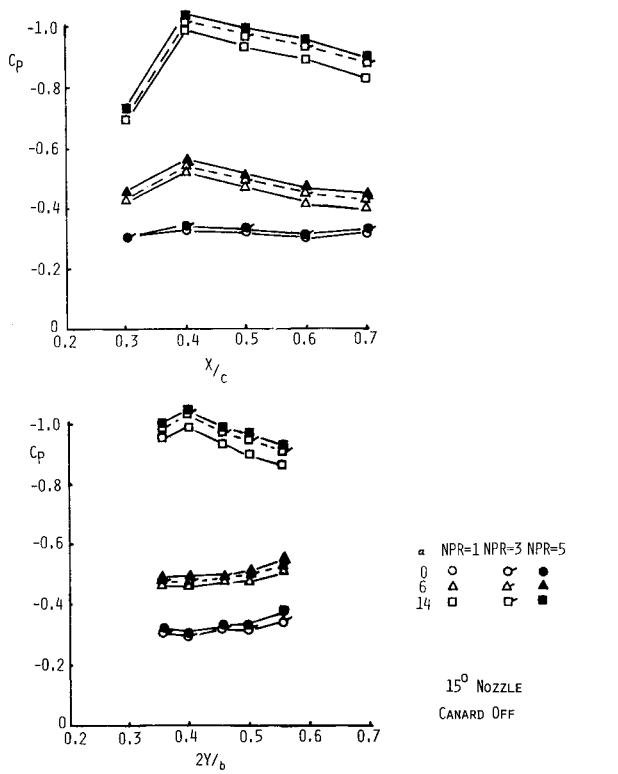

Fig. 11 Wing pressure coefficients, $M=0.6$.

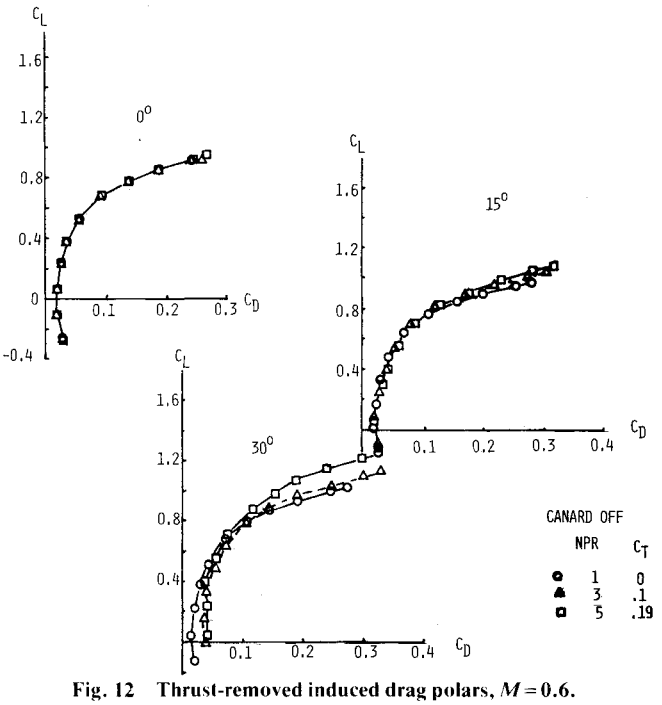

Fig. 12 Thrust-removed induced drag polars, $M=0.6$.

induced aerodynamic components shown in Fig. 10 for $M_\infty=0.6$ indicate that, for a 15 deg vectored nozzle, as the jet flow increases from jet off to nozzle pressure ratios of 3 and 5, the coefficients increase. The induced aerodynamics over the wing are a result of the exhaust nozzle flow changing the pressure distribution around the wing surface. The jet influence provides increased lift, increased drag and a change in pitching moment proportional to the nozzle pressure ratio. The penalty for induced lift from the nozzle vectoring is therefore induced drag and a pitching moment change. This change in wing body aerodynamic coefficients is verified by the upper surface wing pressures ahead of the exhaust nozzle, as indicated in Fig. 11. The pure induced components of the nozzle vectoring changes are shown in Fig. 12. Negligible thrust induced effects are evident for the 0 deg nozzle. The induced effects present for the 15 deg nozzle and 30 deg nozzle are at high lift coefficients only. At low coefficients, the 30 deg nozzle provided a polar worse than that for the 0 and 15 deg nozzles.

A portion of the vectoring drag polar changes is due to the "flap" effect, i.e., a section of the nozzle, turned into the freestream flow, behaves like an aerodynamic control surface. The jet-off drag polar for the three vectored nozzles presented in Fig. 13 indicates that a large portion of the $M_\infty=0.6$ thrust-removed drag polar benefits with nozzle vectoring is due to the "flap" effect. Additional data for $M_\infty=0.3$ indicates that the "flap" effect is a very small contributor to the benefits related to the vectored nozzle. With increased dynamic pressure for $M_\infty=0.6$ rather than $M_\infty=0.3$, the larger contribution of the nozzle surface is not unexpected.

Unless the thrust vector is directed through the aircraft center of gravity, the aircraft will be out of trim when nozzle thrust vectoring is being used. To trim out the vectoring

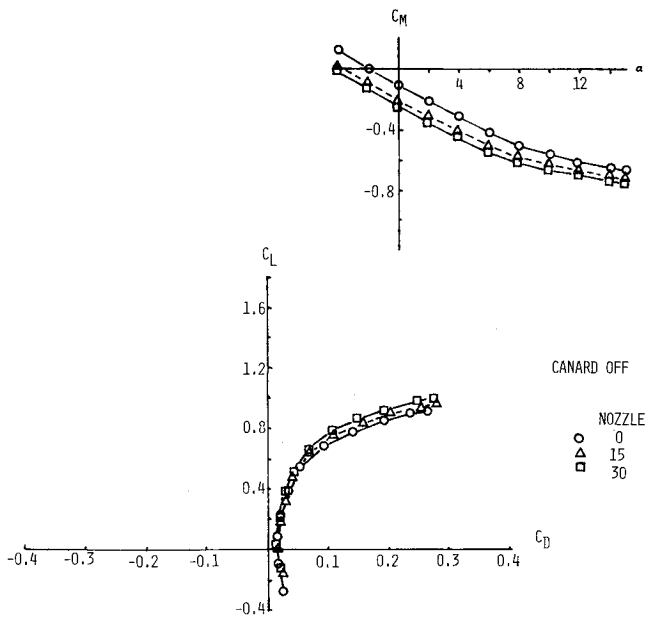

Fig. 13 Jet-off "flap" effect, $M = 0.6$, $NPR = 1$.

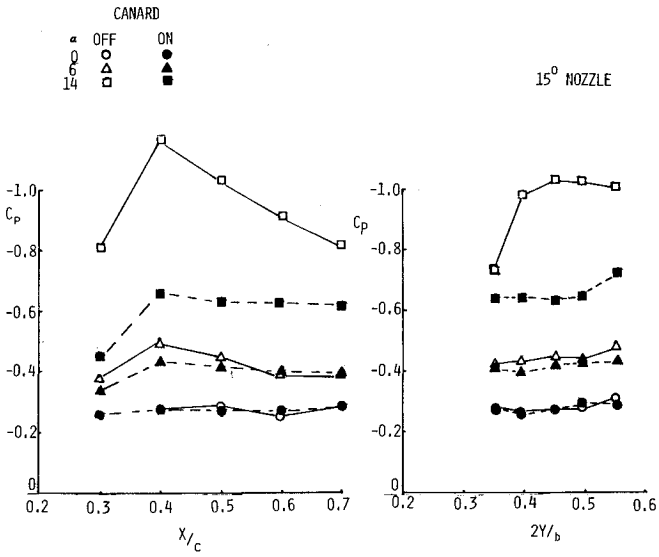

Fig. 15 Wing pressure coefficients, $M = 0.3$, $NPR = 3$.

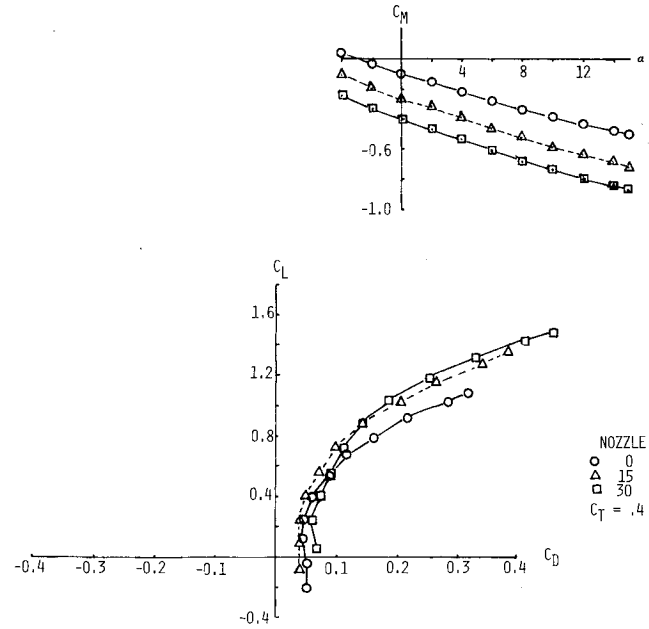

Fig. 14 Thrust-removed drag polar, $M = 0.3$, canard on, $NPR = 3$.

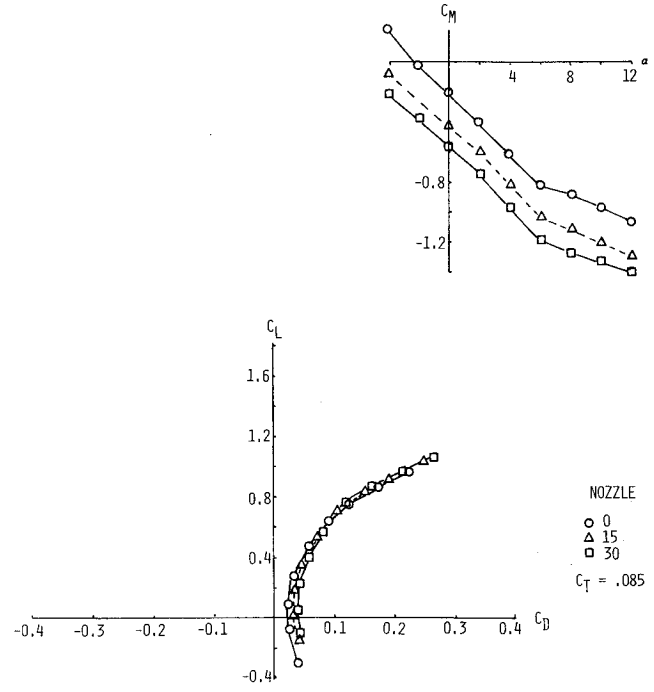

Fig. 16 Thrust-removed drag polar, $M = 0.9$, canard on, $NPR = 5$.

moments, advanced aircraft systems are utilizing relaxed static margin and canards. For selected conditions in this test, a fuselage mounted canard was investigated. In Fig. 14, the thrust-removed drag polar and pitching moment with the canard on are shown. The canard coupled with the 15 deg vectored nozzle gives a better drag polar at low lift coefficients than the 0 deg exhaust nozzle. The 30 deg nozzle crosses over as well, to form a better drag polar at high lift coefficients. The influence of the canard on the wing flowfield and wing pressures is presented in Fig. 15. The canard wake tends to suppress the wing pressures, though the relative level of pressure coefficient change due to induced effects does not appear to be affected. Results not shown indicate that the canard influence for $M_\infty = 0.6$ is similar to that shown for $M_\infty = 0.3$. The canard tends to suppress the wing upper surface pressures such that the total vehicle lift lost on the wing is somewhat offset by the canard lift. It should be noted that any canard effect is configuration dependent. Placement and planform of the canard can be critical in determining canard/wing interactions. The trim drag penalty at high lift coefficients would have to be substantial to negate the vectoring benefits shown.

The effect of the canard on the $M_\infty = 0.9$ data is shown by comparing Figs. 9 and 16. While the upstream canard does change the characteristics of the drag polar and pitching moment, the negligible induced effects shown with the canard off are unchanged with the canard in place.

Conclusions

Based on the data generated and analyzed in this effort, the following conclusions can be made:

1) Thrust-removed drag polars, untrimmed, show benefits for thrust vectoring, especially at high lift coefficients for all Mach numbers presented ($M_\infty = 0.3$ to 0.9).

2) Changes in thrust-removed lift, drag and pitching moment coefficient are due to jet-induced aerodynamics and the "flap" effect of the exhaust nozzle surface turned into the freestream flow. As Mach number increases, the contribution of the induced aerodynamic effects decreases and the contribution of the exhaust nozzle "flap" effect increases.

3) As nozzle pressure ratio increases, the induced effects tend to increase proportionally.

4) Upper surface wing pressure coefficients support the data trends for all exhaust nozzles and test conditions.

5) The trends shown by this data are indicative of the potential of propulsion-induced aerodynamics to improve advanced aircraft systems.

References

[1] Hiley, P.E., Wallace, H.W., Booz, D.E., "Study of NonAxisymmetric Nozzles Installed in Advanced Fighter Aircraft," *Journal of Aircraft*, Vol. 13, Dec. 1976, pp. 1000-1006.

[2] Yoshihara, H., "Transonic Performance of Jet Flaps on an Advanced Fighter Configuration," AFFDL-TR-73-97, July 1973.

[3] Bradley, R.G., Jeffries, R.R., Capone, F.S., "A Vectored-Engine-Over-Wing Propulsive-Lift Concept," presented as Paper 76-917 at the AIAA Aircraft Systems and Technology Meeting, Dallas, Texas, Sept. 1976.

[4] Reubush, D.E., "An Investigation of Induced Drag Reduction Through Over-The-Wing Blowing," presented as Paper 77-884 at the AIAA/SAE 13th Joint Propulsion Conference, Orlando, Fla., July 1977.

[5] Capone, F.J., "Supercirculation Effects Induced by Vectoring a Partial-Span Rectangular Jet," *Journal of Aircraft*, Vol. 12, Aug. 1975, pp. 633-638.

[6] Capone, F.J., "A Summary of Experimental Research on Propulsive-Lift Concepts in the Langley 16-Ft Transonic Tunnel," *Journal of Aircraft*, Vol. 13, Oct. 1976, pp. 803-808.

[7] Buchan, F., "An Investigation of a Two-Dimensional Vectored Nozzle From a Wing Trailing Edge," AFIT/GAE/AA/77D-3, Air Force Institute of Technology, Dec. 1977.

From the AIAA Progress in Astronautics and Aeronautics Series..

AERODYNAMIC HEATING AND THERMAL PROTECTION SYSTEMS—v. 59

HEAT TRANSFER AND THERMAL CONTROL SYSTEMS—v. 60

Edited by Leroy S. Fletcher, University of Virginia

The science and technology of heat transfer constitute an established and well-formed discipline. Although one would expect relatively little change in the heat transfer field in view of its apparent maturity, it so happens that new developments are taking place rapidly in certain branches of heat transfer as a result of the demands of rocket and spacecraft design. The established "textbook" theories of radiation, convection, and conduction simply do not encompass the understanding required to deal with the advanced problems raised by rocket and spacecraft conditions. Moreover, research engineers concerned with such problems have discovered that it is necessary to clarify some fundamental processes in the physics of matter and radiation before acceptable technological solutions can be produced. As a result, these advanced topics in heat transfer have been given a new name in order to characterize both the fundamental science involved and the quantitative nature of the investigation. The name is Thermophysics. Any heat transfer engineer who wishes to be able to cope with advanced problems in heat transfer, in radiation, in convection, or in conduction, whether for spacecraft design or for any other technical purpose, must acquire some knowledge of this new field.

Volume 59 and Volume 60 of the Series offer a coordinated series of original papers representing some of the latest developments in the field. In Volume 59, the topics covered are 1) The Aerothermal Environment, particularly aerodynamic heating combined with radiation exchange and chemical reaction; 2) Plume Radiation, with special reference to the emissions characteristic of the jet components; and 3) Thermal Protection Systems, especially for intense heating conditions. Volume 60 is concerned with: 1) Heat Pipes, a widely used but rather intricate means for internal temperature control; 2) Heat Transfer, especially in complex situations; and 3) Thermal Control Systems, a description of sophisticated systems designed to control the flow of heat within a vehicle so as to maintain a specified temperature environment.

Volume 59—432 pp., 6×9, illus. $20.00 Mem. $35.00 List

Volume 60—398 pp., 6×9, illus. $20.00 Mem. $35.00 List

TO ORDER WRITE: Publications Dept., AIAA, 1290 Avenue of the Americas, New York, N.Y. 10019